

Phase Separation in Concentrated Solutions of Two Homopolymers and a Diblock Copolymer

Čestmír Koňák,* Petr Štěpánek, and Petr Vlček

Institute of Macromolecular Chemistry, Academy of Sciences of the Czech Republic, 162 06 Prague 6, Czech Republic

Robert M. Johnsen

Institute of Physical Chemistry, University of Uppsala, 751 21 Uppsala, Sweden

*Received June 28, 1994; Revised Manuscript Received December 20, 1994**

ABSTRACT: The dynamic behavior of polystyrene (PS) ($M_w = 9.0 \times 10^5$), poly(methyl methacrylate) (PMMA) ($M_w = 1.4 \times 10^6$ or 1.0×10^5), and styrene–methyl methacrylate diblock copolymer (S-*b*-MMA) ($M_w = 8.0 \times 10^4$) mixtures in a solvent isorefractive with PMMA (benzene) was investigated by quasielastic light scattering spectroscopy as a function of temperature and PMMA concentration in the phase separation region. Only two main dynamic modes were present at low PMMA concentrations corresponding to the trace diffusion of PS and S-*b*-MMA visible probes. In the case of PS homopolymer, the probe diffusion coefficient $D_s \approx c^{-2.9}$, which is close to the reptation prediction for self-diffusion of flexible polymers at Θ -conditions, $D_s \approx c^{-3}$. The concentration dependence of D_c for the trace diffusion of S-*b*-MMA also follows a power law but with a smaller exponent ($D_c \approx c^{-2.3}$). With concentrations of PMMA increasing above a threshold concentration, the decay time distribution displayed a complex structure with three main separated bands. The very slow broad mode was related to the phase separation in the mixture and originates from aggregates of probe polymers. The phase separation also appeared on heating in some solutions with appropriate concentration. Experiments have shown that the early stage of the phase separation in the mixtures is mostly due to the aggregation of the high-molecule-weight PS and the low-molecular-weight block copolymer mostly remains molecularly dissolved. Thus, possibly only the late stage of the phase separation process could be influenced by the presence of the diblock copolymer.

Introduction

The importance of polymer blends is evidenced not only by their ubiquitous presence in commercial products in recent years but also by the fact that they prove to be ideal systems for fundamental studies of phase separation phenomena.¹ To improve compatibility between homopolymer A and homopolymer B, it is tempting to employ an AB-type diblock copolymer, such that block A may be compatible with homopolymer A and block B may be compatible with homopolymer B.^{2–4} This “compatibilizer effect” of copolymers is believed to be due to their ability to form microphase morphologies^{5,6} that are thermodynamically stable or to stabilize the thermodynamically unstable macrophase morphologies of the blends A/B.⁷ In the latter case, the diblock copolymer reduces the interfacial tension of the coexisting phases. This reduction in the interfacial tension arises as a result of the tendency of block copolymer molecules to accumulate at the boundary between two immiscible homopolymer phases.^{4,7,8} The question to be answered is how much of the added copolymer is needed to convert the coarse macrophase morphologies produced by the phase separation of blend A/B into fine microphase structures resembling those of the copolymer AB. Recently, it was found⁷ for symmetrical diblock copolymers that the ratio

$$\lambda = V_H/V_{AB}; \quad V_H = V_A = V_B \quad (1)$$

where V_H and V_{AB} are the chain volumes of homopolymers and a copolymer is controlled by the morphologies of the solid blends. Thus, at $\lambda \geq 1$, where the homopolymer chains are longer than those of the diblock copolymer, AB copolymers should form macrophases like a third immiscible homopolymer.⁹ At lower λ ,

copolymers should form micelles as well as interface layers.^{10,11} At the same time the importance for miscibility of the conformational asymmetry ϵ between the A and B monomers was established.¹² ϵ is defined as

$$\epsilon = (\beta_A/\beta_B)^2 \quad (2)$$

where

$$\beta^2 = l_e/6v_0 \quad (3)$$

with l_e being the statistical segment length of the repeating unit and v_0 the segment volume. The more ϵ is different from 1 (greater or less than), the more important are entropic contributions to the interaction parameter χ . Nevertheless, the effect of diblock copolymers on the phase separation process in polymer blends has not yet been clearly established. The interesting role of copolymers in solid blends has motivated studies of solution properties of two homopolymers and a diblock copolymer.¹¹

In the present study, the dynamic behavior of mixtures of poly(methyl methacrylate) (PMMA), polystyrene (PS), and a symmetric styrene–methyl methacrylate diblock copolymer (S-*b*-MMA) in a solvent isorefractive with PMMA (benzene) has been investigated by quasielastic light scattering (DLS) spectroscopy in the phase separation region. A value of $\lambda > 1$ and an off-critical composition of the mixture with a dominant PMMA component was used throughout this study ($\epsilon \approx 1$). Under such conditions it is possible to observe directly the dynamics of only the “visible” probe polymers (PS and S-*b*-MMA) and their aggregates in solution containing “invisible” PMMA polymer. The index-matched system (PMMA/benzene) used has substantially simplified the analysis of DLS data since the contribution of the main polymeric component (PMMA) to the scattered

* Abstract published in *Advance ACS Abstracts*, March 1, 1995.

Table 1. Characteristics of Polymers and a Block Copolymer

polymer	M_w	M_w/M_n
PS	9.0×10^5	≤ 1.10
PMMA	1.43×10^6	1.09
S- <i>b</i> -MMA	8×10^4	~ 1.5

light was substantially suppressed. The main goal of the research is to understand the mechanism of the phase separation in the mixture. The system PS/PMMA alone exhibits a LCST type phase diagram; i.e., it undergoes phase separation upon heating.¹³ Besides the phase separation issues, the trace diffusion of the "visible" homopolymer (PS) and copolymer (S-*b*-MMA) in the polymeric matrix of the "invisible" homopolymer (PMMA) has been studied.

Experimental Section

Polymers and Solvent. High-molecular-weight atactic poly(methyl methacrylate) and polystyrene standards (Polysciences) were used in the study. The poly(styrene-*b*-methyl methacrylate) diblock copolymer was prepared by a two-step anionic copolymerization, initiated with *n*-butyllithium in THF¹⁴ at -40°C . Prior to the addition of MMA, living polystyrene was stabilized with lithium *tert*-butoxide as described in ref 15. The product was characterized by GPC using a column filled with a mixture of Styragel (79911 GP-109 MIX, H-P, U.S.A.) having a separation efficiency in the range of molecular weights 10^3 – 10^6 , with IR and UV (254 nm) detection. The chemical composition, expressed by the molar fraction of styrene units, is 49.4. Molecular characteristics of both the polymers and the copolymer are shown in Table 1.

Benzene (isorefractive solvent for PMMA), reagent grade (Lachema, Czech Republic), was purified and dried before use.

Sample Preparation. Concentrated solutions of PS/PMMA/S-*b*-MMA mixtures were prepared by two different methods:

System 1: The samples were prepared by radical polymerization of methyl methacrylate in benzene with dissolved PS and S-*b*-MMA. The concentration of PS ($M_w = 9.0 \times 10^5$) was $c_s = 1.0 \times 10^{-3}$ g/mL and the concentration of S-*b*-MMA ($M_w = 8.0 \times 10^4$) $c_c = 1.0 \times 10^{-2}$ g/mL. The reaction was initiated with azobis(isobutyronitrile) (10 mg/mL of MMA) and allowed to proceed for 7 days at 50°C in cylindrical light scattering cells. All monomer solutions were first filtered using 0.22- μm filters. By the end of this period, the reaction was complete with a conversion better than 95%. The weight-average molecular weight of PMMA as measured by static light scattering was $M_w \approx 1.0 \times 10^5$.

System 2: The quaternary concentrated solutions of PS/PMMA/S-*b*-MMA/benzene were also prepared by evaporation of the solvent from corresponding dilute solutions. PS ($M_w = 9.0 \times 10^5$) and S-*b*-MMA ($M_w = 8.0 \times 10^4$) were used as probe molecules with concentrations below their crossover concentrations¹⁶ $c_s^* \approx 9.0 \times 10^{-3}$ g/mL and $c_c^* = 3.2 \times 10^{-2}$ g/mL (space filling), respectively. PMMA ($M_w = 1.4 \times 10^6$) with concentrations (c_m) above its crossover concentration, $c_m^* \approx 2.1 \times 10^{-2}$ g/mL, formed the "invisible" polymeric matrix.

Ternary polymer solutions have approximately the same PMMA concentrations and containing only PS or only S-*b*-MMA probe polymers were also prepared by both preparation methods for the sake of comparison.

Static Light Scattering (SLS). Static light scattering measurements were performed with a goniometer equipped with an Ar ion laser (vertically polarized, wavelength $\lambda_0 = 514.5$ nm) in the angular range $\theta = 30$ – 150° . The scattered intensity reported in the different figures of this paper has been normalized by the intensity scattered by benzene at $\theta = 90^\circ$ and corrected for variations of the scattering volume.

Dynamic Light Scattering (DLS). Polarized DLS measurements were made using the apparatus and technique described previously.¹⁷ The laser was a 50-mW He–Ne (633 nm) Metra Blansko model. An ALV 5000, multibit, multi- τ autocorrelator was operated with 32 simultaneous sampling times covering approximately 12 decades in delay time. The

samples were thermostated in a refractive index matching liquid (xylene).

The multi- τ autocorrelation functions were analyzed by inverse Laplace transformation using the REPES¹⁸ method of constrained regularization, which is similar in many respects to the inversion routine CONTIN,¹⁹ to obtain a distribution $\tau A(\tau)$ of decay times τ , according to

$$g^2(t) - 1 = \left[\int_0^\infty A(\tau) \exp(-t/\tau) d\tau \right]^2 \quad (4)$$

where $g^2(t)$ is the measured normalized autocorrelation function of scattered light. REPES directly minimizes the sum of the squared differences between the experimental and calculated intensity time correlation functions using nonlinear programming. This method uses an equidistant logarithmic grid with fixed components (here a grid of 10 components per decade) and determines their amplitudes, $\tau A(\tau)$. From the characteristic decay times τ_i (peak positions of $\tau A(\tau)$) the apparent diffusion coefficients, D_{ai} , were obtained for component i from the equation

$$D_{ai} = 1/\tau_i q^2 \quad (5)$$

where q is the magnitude of the scattering vector ($q = 4\pi n_0 \sin(\theta/2)/\lambda_0$, where n_0 is the refractive index of the solvent and λ_0 the wavelength of light used (632.8 nm)). The diffusion coefficients, D_i , were obtained by extrapolating D_{ai} to zero scattering angle.

Results and Discussion

The dynamic behavior of PMMA/PS/S-*b*-MMA mixtures in a solvent isorefractive with PMMA (benzene) has been investigated by DLS spectroscopy in the phase separation region. The off-critical composition of these mixtures with dominant PMMA as a host (matrix) polymer and with PS and S-*b*-MMA as guest (probe) polymers was used in the present study. The concentrations of both probe polymers were selected in such a way as to obtain comparable contributions to the scattered light. Solutions of polymer mixtures were brought from the one-phase regime into the two-phase region by increasing the PMMA concentration, keeping the temperature constant and the concentration of guest polymers below their c^* , or by increasing the temperature above the binodal temperature, keeping the concentration and composition constant. Let us recall that this system has a LCST type of phase diagram.^{13,20}

Concentration Dependences. According to expectation, the dynamic properties of PMMA/PS/S-*b*-MMA solutions are strongly influenced by the phase separation process. This is demonstrated in Figure 1, where the distribution functions of decay times, $\tau A(\tau)$, are plotted for several PMMA concentrations, c_m (system 1), in the vicinity of the phase separation threshold concentration, $c_{mt} \approx 0.16$ g/mL, as will be determined below. The two distribution functions at lower concentrations ($c_m = 0.1$ and 0.15 g/mL) are typical of dynamic behavior of system 1 in the one-phase region. These distribution functions consist of two well-separated main bands centered at the fast decay time, τ_c , and the slow decay time, τ_s . Both dynamic processes characterized by τ_c and τ_s have a diffusion character (reciprocal values of τ_c and τ_s are linear in q^2). Hence, it was possible to introduce two diffusion coefficients, D_c (fast process) and D_s (slower process). The D_c and D_s diffusion modes are related to the tracer diffusion of the S-*b*-MMA and PS visible probes, respectively. This has been determined by comparison of the distribution functions of the decay times of these quaternary solutions with ternary solutions having close matrix concentrations. The results

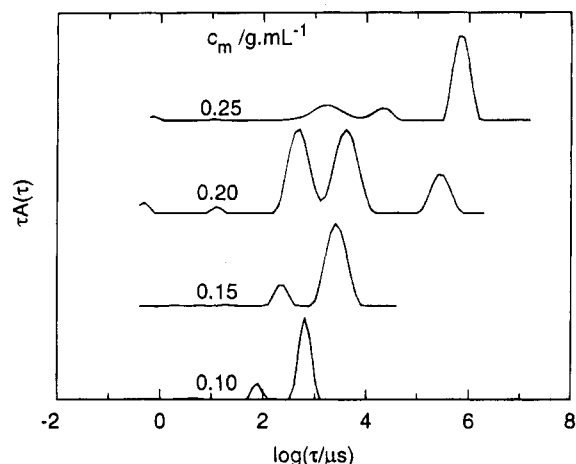


Figure 1. Decay time distributions, $\tau A(\tau)$, for solutions of polymer mixtures (system 1) at various PMMA concentrations c_m . The measurements were done at 25 °C and a scattering angle of 90°.

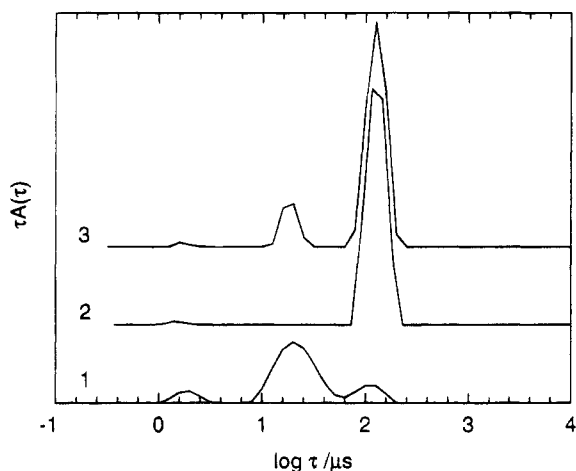


Figure 2. Decay time distributions, $\tau A(\tau)$, of three different solutions (system 2) having the same matrix concentration ($c_m = 4 \times 10^{-3}$ g/mL) containing (1) only S-b-MMA copolymer, (2) only PS polymer, or (3) both PS and S-b-MMA probe polymers.

(system 2) for a solution in the one-phase region ($c_m = 4.0 \times 10^{-3}$ g/mL) are demonstrated in Figure 2. Similar results were obtained for samples with other concentrations including those in the vicinity of the phase separation conditions. Curve 1 corresponds to S-b-MMA copolymer chains only in the invisible PMMA matrix. The very fast small peak, present also on curves 2 and 3, has an almost negligible amplitude and corresponds to the pseudogel diffusion coefficient of the PMMA matrix. The peak on curve 1 located at $\tau \approx 100 \mu s$ ($\log \tau \approx 2$) has also a very small amplitude and can be assigned to copolymer aggregates which are formed due to the presence of stereoregular sequences in PMMA blocks of the copolymer used.²¹ Curve 2 in Figure 2 was only obtained with PS chains mixed with the PMMA matrix and shows a single dominant peak of the diffusion of these chains. Finally, curve 3 was obtained in a solution where both the PS and the copolymer were added to the "invisible" PMMA matrix. Both components can be easily separated in the spectra and identified as corresponding to the PS diffusion (slow mode) and copolymer diffusion (fast mode). The scattering amplitude of the cooperative diffusion mode of the "invisible" PMMA matrix is very weak and can be found as a small peak in the short-time region (2–5 μs) of Figure 1. The fact that we can observe a cooperative

mode for the index-matched system is obviously due to its coupling to the tracer diffusion of probe polymers similarly as it is in PMMA/PS/toluene ternary solutions.²² This effect was theoretically predicted by the random phase approximation and discussed recently.²³ Some implications of this theory were experimentally tested by DLS experiments using a variety of ternary mixtures of two polymers and solvents isorefractive with one of them.^{22,24}

The samples with $c_m = 0.2$ and 0.25 g/mL were turbid even after intensive mixing, and the macroscopic phase separation was observed after several weeks. Therefore, we classified this sample to be already in the two-phase regime. The corresponding decay time distributions in Figure 1 become broader and displayed a complex structure with three main separated bands. These distribution functions were measured just after an intensive mixing of the sample and corresponds to nonequilibrium conditions. Thus, the very slow broad mode can be related to the phase separation in the mixture and comes from aggregation of visible probe polymers. This interpretation is further supported by temperature measurement in the following section. The onset of aggregation for system 1 has been found to be between $c_{mt} = 0.15$ and 0.16 g/mL. Figure 1 shows that the ratio of scattering amplitudes A_s/A_c decreases with increasing concentrations. Thus, $A_s > A_c$ at $c_m = 0.1$ and 0.15 g/mL, $A_s \sim A_c$ at $c_m = 0.2$ g/mL, and obviously $A_s < A_c$ at $c_m = 0.25$ g/mL. This is, in our opinion, due to preferential aggregation of PS macromolecules in the early stage of the phase separation in the mixtures under study. A decrease in the number of free PS macromolecules is reflected in a decrease in A_s and consequently in a decrease in A_s/A_c . The S-b-MMA block copolymer probably forms a third macrophase in the late stage of the phase separation process^{9,11} and/or remains in solution. Unfortunately, this process cannot be followed by DLS spectroscopy because the copolymer aggregation is masked by PS aggregation. In other words, only the early stage of the phase separation may be successfully studied by DLS.

Similar dynamic behavior was observed in system 2 with the only difference that the onset of aggregation was observed at lower PMMA concentrations ($c_{mt} \approx 5.4 \times 10^{-2}$ g/mL) than in system 1 ($c_{mt} \approx 0.16$ g/mL). This observation clearly shows the effect of molecular weight on PS-PMMA miscibility, a decrease in the miscibility with an increase in the molecular weight of the PMMA matrix. This is in qualitative agreement with the Flory-Huggins theory for binary systems.¹³

Besides the phase separation effects, valuable information on tracer diffusion of the S-b-MMA block copolymer and the PS homopolymer in the PMMA matrix was obtained. To interpret these results, log-log plots of D_c and D_s versus c_m are shown in Figures 3 and 4 for systems 1 and 2, respectively. From Figure 4 we can see two distinct scaling regimes for tracer diffusion coefficients D_c and D_s . For $c_m < c_m^*$, (c_m^* is the crossover concentration) we find that D_c is practically independent of c_m and D_s decreases only slightly with increasing c_m . This is in agreement with the well-known behavior of polymers in dilute solutions in a thermodynamically good solvent.²² For $c_m > c_m^*$, close to the threshold PMMA concentration c_{mt} both tracer diffusion coefficients decrease very rapidly with increasing c_m . D_s approaches the power-law dependence $D_s \sim c_m^{-3}$ at higher PMMA concentrations. The power-law dependence with an exponent of 2.9 was found also for system

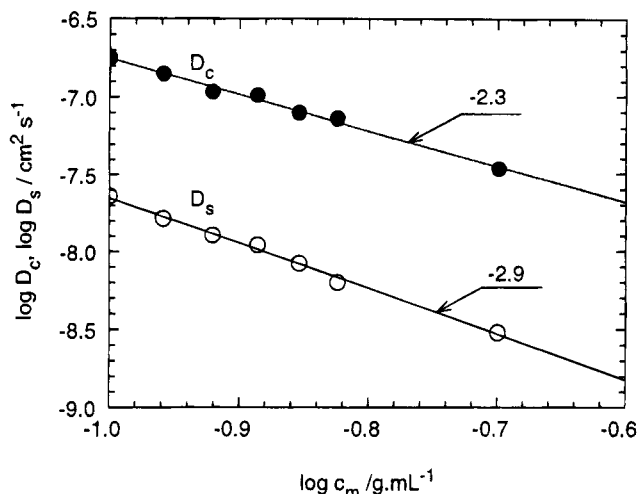


Figure 3. Log-log plot for the fast D_c and slow D_s diffusion coefficients versus the matrix concentration, c_m (system 1).

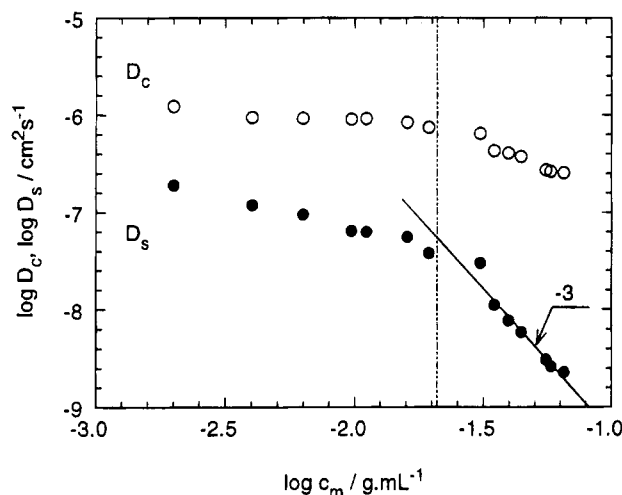


Figure 4. Log-log plot for the fast D_c and slow D_s diffusion coefficients versus the matrix concentration, c_m (system 2).

1 (see Figure 3). Thus, for $c_m^* < c_m < c_{mt}$ the dynamic behavior of the probe PS polymer is close to the reptation prediction for the case when the Stokes-like friction is assumed at Θ conditions,^{25,26} $D_s \sim c_m^{-3}$. These experimental results are in accord with those in ref 27, where the concentration dependence of the self-diffusion coefficient D_s is measured by forced Rayleigh scattering for polystyrene in a Θ -solvent. The c_m dependence of the trace diffusion of S-*b*-MMA copolymer above c_m^* is not so pronounced as in the case of PS. We have found a power-law dependence of D_c with a concentration exponent of -2.3 for system 1 (Figure 3). The absolute value of this exponent is larger than that predicted for flexible homopolymers in a thermodynamically good solvent (1.75) and smaller than that for Θ -solvents (3). This result seems to reflect a complex interaction of the block copolymer macromolecules with the homopolymer matrix. Unfortunately, to our knowledge, this problem has not been analyzed theoretically yet.

Temperature Dependences. The phase separation appears on heating of concentrated solutions with c_m just below c_{mt} . The static light scattering data represented by the q^2 dependence of the reciprocal value of the scattered intensity, $(I_s(q))^{-1}$, are given for several temperatures in the temperature range 20–35 °C in Figure 5. The measurement temperature was gradually increased by steps, and samples were equilibrated 20

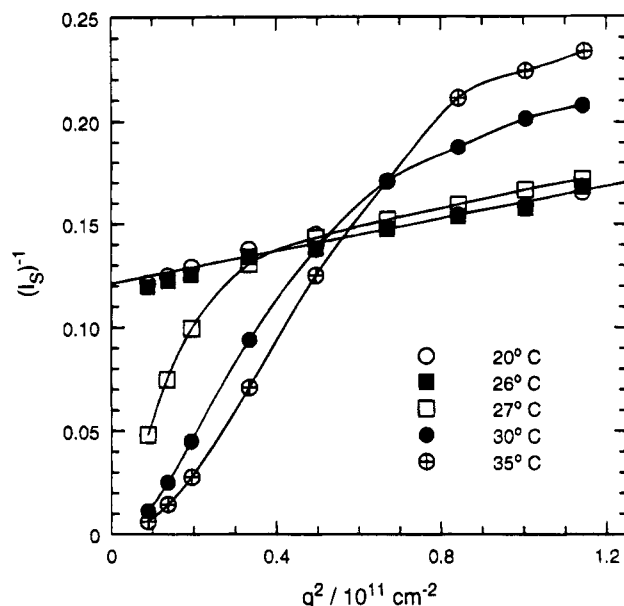


Figure 5. q^2 dependence of the reciprocal value of the scattering intensity, $(I_s(q))^{-1}$, for the solution with $c_m = 0.15$ g/mL measured at various temperatures as indicated.

min before DLS or SLS was measured. A simple linear dependence of $(I_s(q))^{-1}$ on q^2 was observed for temperatures below 26 °C. The apparent radius of gyration $R_g \approx 50$ nm was estimated from the slope of the q^2 dependence of $(I_s(q))^{-1}$ and the zero scattering angle value of $I_s(0)$. The R_g value is approximately 1.5 times higher than the unperturbed radius of PS molecules in cyclohexane. It is plausible to suppose that the sample at $T \leq 26$ °C is still in the one-phase region. At temperatures $T \geq 27$ °C the q^2 dependence of $(I_s(q))^{-1}$ drastically changes. The scattered intensity, $I_s(q)$, increases at low q values and decreases at higher q values. The increase of $I_s(q)$ at low q values can be explained by the appearance of aggregates in the two-phase region and the decrease of $I_s(q)$ at higher q by a decrease of concentration of free probe molecules due to their aggregation. Thus, the threshold temperature, T_t , between the one- and two-phase regions is localized between 26 and 27 °C. The above interpretation is further emphasized by DLS measurements in Figure 6, where a series of decay time distribution functions is shown for several temperatures below ($T = 25$ °C) and above ($T \geq 30$ °C) the phase separation threshold, T_t , for the sample with $c_m = 0.15$ g/mL (system 1). Only two self-diffusion modes are present at 25 °C and formation of the third slow mode of aggregates starts at higher temperatures. The temperature dependence of the scattering amplitude of aggregates, A_a , evaluated from data of Figure 6 is plotted in Figure 7 for the sample with $c_m = 0.15$ g/mL. A threshold temperature $T_t = 29$ °C was roughly estimated by extrapolating A_a to zero (see Figure 7). This value of T_t corresponds to that obtained in SLS measurements.

For system 2 and for the sample with $c_m = 5.4 \times 10^{-2}$ g/mL, a weak aggregation has already been found at 25 °C (results not shown) which increased on heating although not as intensively as in system 1. Probably, the kinetics of the phase separation in the high-molecular-weight PMMA matrix (system 2) is slower than that in the low-molecular-weight matrix of system 1.

Figure 8 shows that the scattering amplitude of PS (A_s) decreases faster than that of the copolymer S-*b*-

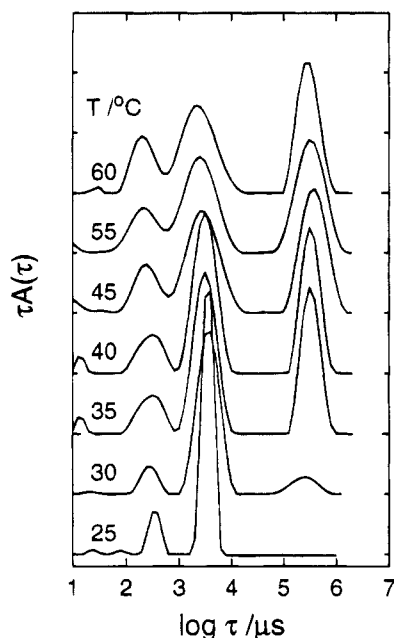


Figure 6. Decay time distributions, $\tau A(\tau)$, for the solutions with $c_m = 0.15$ g/mL (system 1) measured at a scattering angle of 90° and various temperatures as indicated.

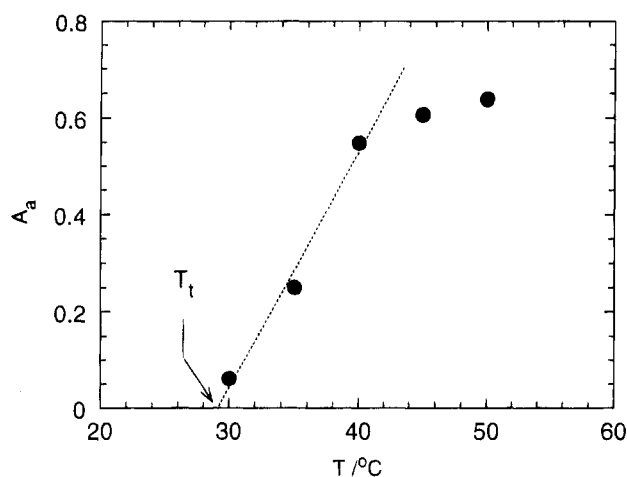


Figure 7. Temperature dependence of the scattering amplitude of aggregates, A_a , for the sample with PMMA concentration of 0.15 g/mL. Data were evaluated from Figure 6.

MMA (A_c) on heating. This is in agreement with the results on the concentration dependence of the dynamic behavior presented in the previous section, and it is again due to preferential aggregation of PS macromolecules in the early stage of the phase separation. This finding is indirectly supported by a phase separation study in corresponding ternary solutions. While S-*b*-MMA copolymer is soluble above c_{mt} for the quaternary solution, the phase separation of PS is found to be approximately at the same concentration and in a similar temperature range as in the case of the quaternary solutions. Since the phase separation conditions of the off-critical samples used in this study are strongly c_m dependent (more pronounced effect than temperature), it is practically impossible to compare quantitatively the transition temperatures between ternary solutions containing PS and quaternary solutions. Thus, e.g., a decrease of c_m by 1 wt % from 0.15 to 0.14 g/mL evokes at T_t increase from 25 °C to somewhere above the boiling temperature of benzene (80.1 °C). To address this issue, a new experimental study of the effect of block copolymers on the phase separation in poly-

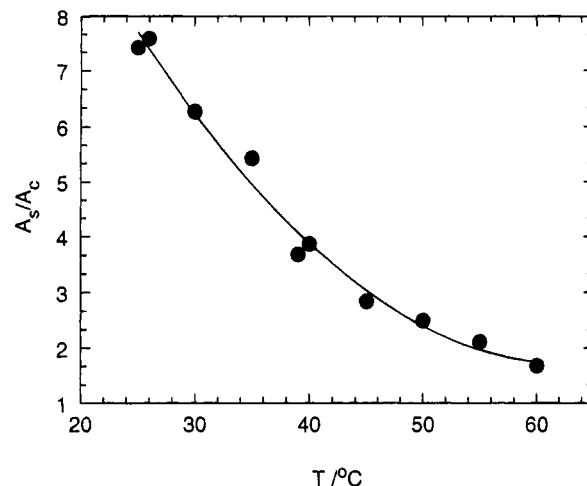


Figure 8. Temperature dependence of the scattering amplitude ratios, A_s/A_c evaluated from the $\tau A(\tau)$ distributions in Figure 6.

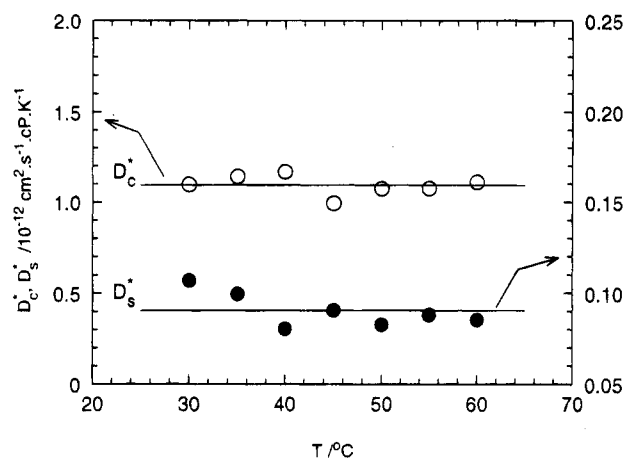


Figure 9. Temperature dependence of reduced diffusion coefficients D_c^* and D_s^* . Diffusion coefficients were evaluated from the distributions in Figure 6.

meric mixtures is in progress with critical samples where the effect of concentration variations is minimized. Nevertheless, the above results clearly implicate that the S-*b*-MMA copolymer is still well soluble in the PMMA matrix at c_{mt} concentrations and that the phase separation induced by an increase in temperature is mostly due to aggregation of high-molecular-weight PS macromolecules.

For the temperature dependence of the tracer diffusion coefficients we have found that $D_c \sim D_s \sim T/\eta$, where η is the solvent viscosity; Figure 9 shows the reduced diffusion coefficient $D_i^* = D_i\eta/T$ ($i = c, s$) for both the PS and S-*b*-MMA components which is, within experimental error, independent of temperature. An absence of critical slowing down in the samples under study demonstrates that the off-critical composition used is really very far away from critical conditions. No critical slowing down near T_t is observed as expected since the samples used have off-critical compositions.

Conclusion

In conclusion, we can point out that the early stage of the phase separation in the quaternary solutions under study is mostly characterized by the aggregation of the high-molecular-weight ($M_w = 9.0 \times 10^5$) PS macromolecules. Thus, only the late stage of the phase separation process could be influenced by the presence

of the diblock copolymer. This result is of basic importance for the understanding of the compatibilizing effect of copolymers in polymer blends. A more active role of block copolymers at the early stage of the separation process can be expected for diblock copolymers having block molecular weights larger than those of the homopolymers in the mixture ($\lambda < 1$). To verify this hypothesis new experiments are in progress on PS/PMMA/S-*b*-MMA/benzene mixtures.

Acknowledgment. We gratefully acknowledge the support of this work by the U.S.-Czech Science and Technology Program under Grant 92053, by the Grant Agency of the Academy of Sciences of the Czech Republic under Grant 450416, and by the Grant Agency of the Czech Republic under Grants 203/93/1063 and 203/94/0817.

References and Notes

- (1) Olabisi, O.; Robeson, L. M.; Shaw, M. T. *Polymer-Polymer Miscibility*; Academic Press: New York, 1979.
- (2) Paul, D. In *Polymer Blends*; Paul, D., Ed.; Academic Press: New York, 1978; Vol. 2, Chapter 12.
- (3) Tanaka, H.; Hasegawa, H.; Hashimoto, T. *Macromolecules* **1991**, *24*, 240.
- (4) Park, D. W.; Roe, R. J. *Macromolecules* **1991**, *24*, 5324.
- (5) Bates, F. S. *Science* **1991**, *251*, 898.
- (6) Thomas, E.; Alward, D.; Kinning, D.; Martin, D.; Handlin, D.; Fetters, L. *Macromolecules* **1986**, *19*, 2197.
- (7) Jiang, M.; Xie, H. *Prog. Polym. Sci.* **1991**, *16*, 977.
- (8) Leibler, L. J. *Macromolecules* **1982**, *15*, 1283.
- (9) Löwenhaupt, B.; Hellmann, G. P. *Polymer* **1991**, *32*, 1065.
- (10) Löwenhaupt, B.; Hellmann, G. P. *Colloid Polym. Sci.* **1990**, *268*, 885.
- (11) Löwenhaupt, B.; Hellmann, G. P. *Colloid Polym. Sci.* **1994**, *272*, 121.
- (12) Geblsen, M. D.; Bates, F. S. *Macromolecules*, in press.
- (13) Lau, W. W. Y.; Burns, C. M.; Huang, R. Y. M. *J. Appl. Polym. Sci.* **1984**, *29*, 1531.
- (14) Fetters, L. J.; Young, R. N. *ACS Symp. Ser.* **1981**, *166*, 95.
- (15) Vlček, P.; Lochmann, L.; Otoupalová, J. *Makromol. Chem., Rapid Commun.* **1992**, *13*, 163.
- (16) Aharoni, S. M. *J. Macromol. Sci., Phys.* **1978**, *B15*, 347.
- (17) Koňák, Č.; Štěpánek, P.; Sedláček, B. *Czech. J. Phys.* **1984**, *A34*, 497.
- (18) Štěpánek, P. In *Dynamic Light Scattering: The Method and Some Applications*; Brown, W., Ed.; Oxford University Press: New York, 1993; Chapter 4.
- (19) Provencher, S. W. *Makromol. Chem.* **1979**, *180*, 201.
- (20) Geveke, D. J.; Danner, R. P. *J. Appl. Polym. Sci.* **1993**, *47*, 565.
- (21) Koňák, Č.; Vlček, P.; Bansil, R. *Macromolecules* **1993**, *26*, 3717.
- (22) Koňák, Č.; Tuzar, Z.; Jakeš, J. *Polymer* **1990**, *31*, 1866.
- (23) Benmouna, M.; Benoit, H.; Duval, M.; Akcasu, A. Z. *Macromolecules* **1987**, *20*, 1107.
- (24) Giebel, L.; Borsali, R.; Fischer, E. W.; Meier, G. *Macromolecules* **1990**, *23*, 4054.
- (25) de Gennes, P.-G. *Scaling Concepts in Polymer Physics*; Cornell University Press: Ithaca (NY) and London, 1979.
- (26) Doi, M.; Edwards, S. F. *The Theory of Polymer Dynamics*; Clarendon Press: Oxford, 1986.
- (27) Deschamps, H.; Leger, L. *Macromolecules* **1986**, *19*, 2760.

MA946018+